The Aharonov-Bohm effect in double- and single-slit diffraction

1989 J. Phys. A: Math. Gen. 22 3605

(http://iopscience.iop.org/0305-4470/22/17/024)

J. Phys. A: Math. Gen. 22 (1989) 3605-3611. Printed in the UK

The Aharonov–Bohm effect in double- and single-slit diffraction

Daniel Shapiro† and Walter C Henneberger

Department of Physics, Southern Illinois University, Carbondale, IL 62901-4401, USA

Received 31 January 1989

Abstract. Single- and double-slit diffraction patterns are obtained by means of path integrals. The slit function is taken to be unity. This permits the study of the single-slit case as a limit of the double-slit case when the slit width is equal to the slit separation. Introduction of a whisker of flux at the midpoint of the space between slits gives the Aharonov-Bohm shift. In the case of a wide single slit, one obtains conditions approaching those postulated in calculations similar to the scattering calculation of Aharonov and Bohm.

1. Introduction

The Aharonov-Bohm (AB) effect is a shift in an interference pattern that occurs when two distinct paths are open to an electron moving from a cathode to a screen, when a whisker of magnetic flux is inserted into an inaccessible region between the paths [1]. In experiments, the two paths are produced electrostatically [2, 3, 4]. For the sake of discussion of theory, it is convenient to consider paths produced by a double-slit system.

The mathematical treatment that has had the most success in producing results that agree with experiment is the Feynman path-integral method [5, 6]. Much work has been done on applications of path integrals to the AB effect over the years [7-10].

In this paper, we apply the Feynman path-integral method to a realistic double-slit system with a whisker of flux in the space between the slits. Since a slit function of unity is assumed, one may vary the parameters of the problem (slit width and separation) to cover any case of interest. In particular, one can consider the case in which the space between the slits is zero. This results in a single slit with the whisker of flux at its centre. If one now makes the resulting single slit very wide, one can approximate the conditions assumed in so-called Aharonov-Bohm scattering calculations. While the effect of the slit edges is still evident, the wider one makes the slit, the more nearly one approaches the conditions of the AB scattering problem.

2. The single slit

We begin by considering the single-slit problem, following Feynman and Hibbs [11]. The situation is shown in figure 1.

† Present address: Department of Biophysics, University of California, Berkeley, CA 94720, USA.

0305-4470/89/173605+07$02.50

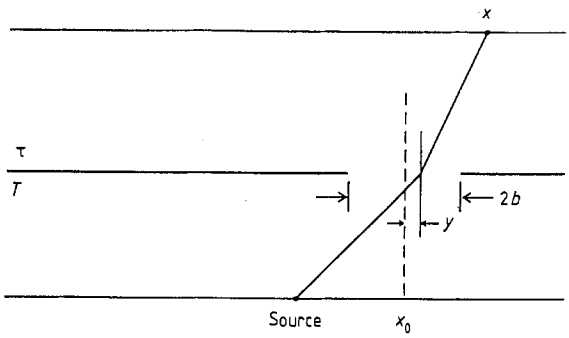

Figure 1. Single-slit geometry.

An electron leaving the source at $t=0$ has an amplitude $\psi(x)$ for arriving at the point $x+x_0$ on the screen at time $T+\tau$ given by

$$\psi(x)=\int_{-b}^{b} K(x+x_0,\, T+\tau;\, x_0+y,\, T)K(x_0+y,\, T;\, 0,\, 0)\,\mathrm{d}y. \tag{1}$$

In (1), T is the time taken for the particle to go from the source at $x=0$ to the plane of the slit, and τ is the time to proceed from the slit plane to the screen. The slit has width $2b$. The kernel for a free particle going from b to a is given by

$$K(b,a)=\left(\frac{2\pi \mathrm{i}\hbar(t_b-t_a)}{m}\right)^{-1/2}\exp\left(\frac{\mathrm{i}m(x_b-x_a)^2}{2\hbar(t_b-t_a)}\right). \tag{2}$$

Applying (2) to (1), completing the squares and rearranging terms gives

$$\psi(x)=A\,\mathrm{e}^{\mathrm{i}\delta}\left\{\int_{-b}^{b}\cos\left[\frac{m}{2\hbar}\left(\frac{1}{T}+\frac{1}{\tau}\right)\left(y+\frac{\tau x_0-Tx}{T+\tau}\right)^2\right]\mathrm{d}y \right.$$
$$\left.+\mathrm{i}\int_{-b}^{b}\sin\left[\frac{m}{2\hbar}\left(\frac{1}{T}+\frac{1}{\tau}\right)\left(y+\frac{\tau x_0-Tx}{T+\tau}\right)^2\right]\mathrm{d}y\right\} \tag{3}$$

with

$$A=\frac{m}{2\pi \mathrm{i}\hbar\sqrt{T\tau}}$$

and

$$\delta=\frac{m}{2\hbar}\left[\left(\frac{x^2}{\tau}+\frac{x_0^2}{T}\right)-\left(\frac{1}{T}+\frac{1}{\tau}\right)\left(\frac{\tau x_0-Tx}{T+\tau}\right)^2\right]=\frac{m}{2\hbar}\,\frac{(x+x_0)^2}{(T+\tau)}. \tag{4}$$

The integrals are expressible in terms of Fresnel integrals

$$\int_0^b \begin{matrix}\cos\\ \sin\end{matrix}(uy^2)\,\mathrm{d}y=\sqrt{\frac{\pi}{2u}}\begin{matrix}C\\ S\end{matrix}\left(\sqrt{\frac{2u}{\pi}}\,b\right). \tag{5}$$

We set $u=(m/2\hbar)((1/T)+(1/\tau))$ and make a change of variable: $y'=y+(\tau x_0-Tx)/(T+\tau)$. The final result is

$$\psi(x)=\frac{\mathrm{i}}{2}\sqrt{\frac{m}{\hbar\pi(T+\tau)}}\,\mathrm{e}^{\mathrm{i}\delta}\{[C(u_1)-C(u_2)]+\mathrm{i}[S(u_1)-S(u_2)]\} \tag{6}$$

where

$$u_1 = \frac{x - \tau v_0 - b(1+\tau/T)}{\sqrt{(\pi\hbar\tau)/m}(1+\tau/T)^{1/2}}$$
$$u_2 = \frac{x - \tau v_0 + b(1+\tau/T)}{\sqrt{(\pi\hbar\tau)/m}(1+\tau/T)^{1/2}} \tag{7}$$

and $v_0 \equiv x_0/T$. The probability distribution at the screen is thus proportional to

$$|\psi|^2 = \frac{m}{4\pi\hbar(T+\tau)}\{[C(u_1)-C(u_2)]^2+[S(u_1)-S(u_2)]^2\}. \tag{8}$$

3. The double slit

One may generalise the result of the previous section by writing the double-slit amplitude as a superposition of single-slit amplitudes (figure 2)

$$\psi(x) = \psi^+(x) + \psi^-(x). \tag{9}$$

$\psi^+(x)$ and $\psi^-(x)$ are obtained from (8) by a shift of origin. The total amplitude is

$$\psi(x) = K\,\mathrm{e}^{\mathrm{i}\delta^+}(C^+ + \mathrm{i}S^+) + K\,\mathrm{e}^{\mathrm{i}\delta^-}(C^- + \mathrm{i}S^-) \tag{10}$$

with

$$K = \frac{1}{2}\left(\frac{m}{\mathrm{i}\hbar\pi(T+\tau)}\right)^{1/2}$$
$$\delta_\pm = \frac{m}{2\hbar}\left[\frac{(x \mp x_0)^2}{\tau} + \frac{x_0^2}{T} - \left(\frac{1}{T}+\frac{1}{\tau}\right)\left(\frac{\pm\tau x_0 - T(x \mp x_0)}{T+\tau}\right)^2\right]$$
$$C^\pm = C(u_1^\pm) - C(u_2^\pm)$$
$$S^\pm = S(u_1^\pm) - S(u_2^\pm) \tag{11}$$
$$u_1^\pm = \frac{x \mp x_0 \mp \tau v_0 - b(1+\tau/T)}{\sqrt{\pi\hbar\tau/m}(1+\tau/T)^{1/2}}$$
$$u_2^\pm = \frac{x \mp x_0 \mp \tau v_0 + b(1+\tau/T)}{\sqrt{\pi\hbar\tau/m}(1+\tau/T)^{1/2}}.$$

In the case under consideration $\psi_+ = \delta_- = (m/2\hbar)x^2/(T+\tau)$ so that the distribution is

$$P(x) = K^2[(C^+)^2+(S^+)^2+(C^-)^2+(S^-)^2+2(C^-C^+ + S^-S^+). \tag{12}$$

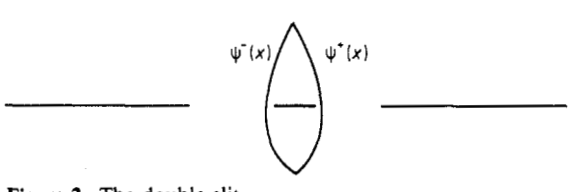

Figure 2. The double slit.

4. Aharonov–Bohm effect

In order to study the Aharonov-Bohm effect, we utilise the Feynman propagator for an electron in an external vector potential. The Lagrangian is now

$$L = L_0 + \frac{e}{c}\boldsymbol{v}\cdot\boldsymbol{A} \tag{13}$$

where L_0 is the free particle Lagrangian.

The propagator is now given by

$$K'(x+x_0,\ T+\tau,\ x_0+y,\ T) = \int_{x_0+y}^{x_0+x} \mathrm{D}^3(x)\exp\left[\frac{\mathrm{i}}{\hbar}\int_T^{\tau}\mathrm{d}t\left(L_0+\frac{e}{c}\boldsymbol{v}\cdot\boldsymbol{A}\right)\right]. \tag{14}$$

Since $\boldsymbol{v}\cdot\boldsymbol{A}\,\mathrm{d}t = \boldsymbol{A}\cdot\mathrm{d}\boldsymbol{x}$, (14) is simply the free particle propagator multiplied by the Dirac phase factor

$$\exp\left(\frac{\mathrm{i}e}{\hbar c}\int_{x_0+y}^{x_0+x}\mathrm{d}\boldsymbol{x}\cdot\boldsymbol{A}\right) \tag{15}$$

It is straightforward to show that the amplitude for an electron to arrive at a point x on the screen is

$$\psi(x) = K\,\mathrm{e}^{\mathrm{i}\delta'_+}(C^+ + \mathrm{i}S^+) + K\,\mathrm{e}^{\mathrm{i}\delta'_-}(C^- + \mathrm{i}S^-) \tag{16}$$

with $\delta'_+ - \delta'_- = e\Phi/\hbar c$. Here Φ is the flux embedded in a whisker at $y = 0$.

The final result is

$$P(x) = K^2[(C^+)^2 + (S^+)^2 + (C^-)^2 + (S^-)^2]$$
$$+ 2K^2\cos\left(\frac{e\Phi}{\hbar c}\right)[C^-C^+ + S^-S^+] + 2K^2\sin\left(\frac{e\Phi}{\hbar c}\right)[S^-C^+ - C^-S^+]. \tag{17}$$

5. Results

Results (equation (17)) were computed by means of a FORTRAN program that was based on Romberg's method [12]. Figure 3 shows the probability distribution in arbitrary units against distance for slit widths of two microns ($b = 1.0\times10^{-6}$ m) and slit separation of 10 microns ($x_0 = 5\times10^{-6}$ m). The distance from the source to the slits is equal to that from the slits to the screen. The symmetric graph in figure 3 corresponds to no magnetic flux. The graph is a normal double-slit diffraction pattern. The other graph of figure 3 corresponds to a phase $e\Phi/\hbar c = \pi/2$. This pattern is shifted and is asymmetric about the origin. This is in agreement with all previous computations of the AB effect using the Feynman path integral method, and is in contrast to scattering calculations, such as the original computation by Aharonov and Bohm [13], which gives a symmetric scattering cross section.

Figures 4(a) and 4(b) correspond more closely to experimental conditions. Here the slit separation is relatively large ($x_0 = 1.0\times10^{-4}$ m, $b = 5\times10^{-6}$ m). The envelope of a single-slit pattern is easily seen. One notes that the distribution in figure 4(b) is shifted in a manner similar to that of figure 3 when $e\Phi/\hbar c = \pi/2$. The probability distribution never falls to zero in these cases, except at the ends of the distribution.

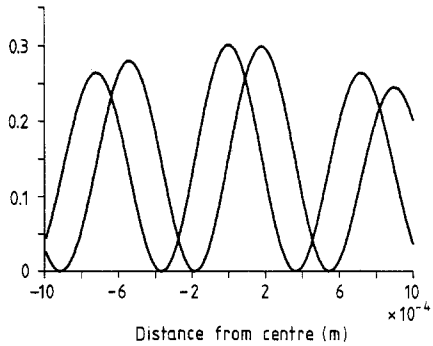

Figure 3. Probability distribution in arbitrary units against distance from the midpoint of the slit system. $b = 10^{-6}$ m, $x_0 = 5 \times 10^{-6}$ m, $T = 10^{-5}$ s, $\tau = 10^{-5}$ s. The symmetric graph corresponds to zero flux; the other to $e\Phi/c\hbar = \pi/2$.

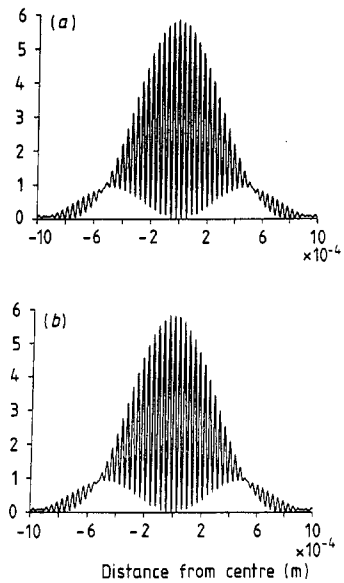

Figure 4. (*a*) Zero flux distribution for $b = 5 \times 10^{-6}$ m, $x_0 = 10^{-4}$ m, $T = 10^{-5}$ s, $\tau = 10^{-5}$ s. (*b*) Aharonov-Bohm shift for $e\Phi/c\hbar = \pi/2$.

An interesting case is the limit as the two slits merge into a single slit ($x_0 = b$). In this case, we have a single slit with a whisker of flux at the centre of the slit. The results are shown in figure 5 for $b = x_0 = 10^{-6}$ m. The zero-flux case gives the single-slit diffraction pattern, as expected. This is shown in the symmetric graph. The case with $e\Phi/c\hbar = \pi/2$ shows a shifted pattern similar to that of the double slit.

Finally, we approach the conditions assumed in the calculation of Aharonov-Bohm scattering [1]. We pass to the case of a whisker of flux at the centre of a very large slit (figures 6(*a*) and 6(*b*)), where $b = x_0 = 1.0 \times 10^{-4}$ m, and figures 7(*a*) and 7(*b*) (where $b = x_0 = 1.0$ mm). In these last graphs, we see clearly the diffraction pattern of the slit edge. In the case $e\Phi/c\hbar = \pi/2$, we see that the asymmetry of the interference pattern persists, and the pattern itself is superimposed on a non-vanishing background.

In order to compare this result with the scattering cross section of Aharonov and Bohm, it is necessary to pass to the Fraunhofer limit (separation between source and

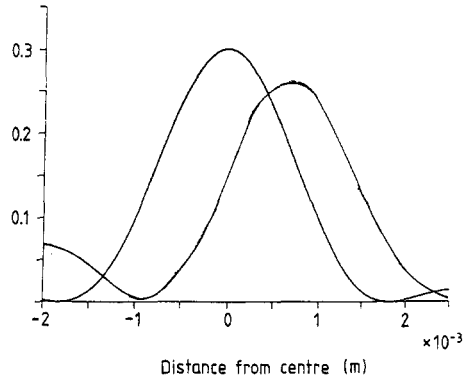

Figure 5. Zero flux single-slit diffraction. $b = x_0 = 10^{-6}$ m, $\tau = T = 10^{-5}$ s (symmetric graph); Aharonov-Bohm shift for the same parameters. The flux whisker is at the centre of the slit; $e\Phi/c\hbar = \pi/2$.

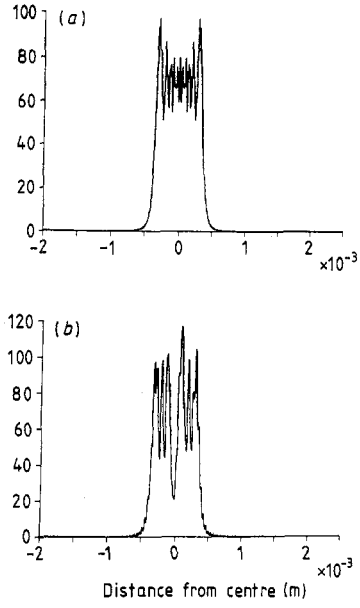

Figure 6. (*a*) Zero flux single-slit diffraction. $b = x_0 = 10^{-4}$ m, $T = \tau = 10^{-5}$ s. (*b*) Aharonov-Bohm shift for the same parameters with $e\Phi/c\hbar = \pi/2$.

screen becoming extremely large, maintaining the slit equidistant from both). In this way, the wave incident upon the slit is very nearly plane, as in the AB computation. In the case of a wide slit, one may use geometrical optics. It is clear that the diffraction pattern of the slit edge lies along a straight line from the source to the slit edge. Since the slit lies halfway between source and screen, by similar triangles the entire diffraction pattern occupies a length that is (apart from some fuzziness) twice the size of the slit width. The Aharonov-Bohm disturbance occupies roughly a quarter of this total length on the screen. The size of the diffraction pattern can never increase significantly, since it is dominated by geometrical considerations. Hence, in the Fraunhofer limit, the angle subtended by the disturbance at the slit must approach zero. It is the subtended

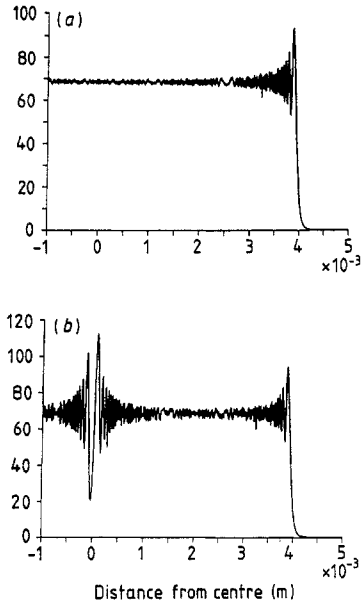

Figure 7. (*a*) Zero flux single-slit diffraction. $b = x_0 = 10^{-3}$ m, $T = \tau = 10^{-5}$ s. (*b*) Aharonov-Bohm shift for the same parameters with $e\Phi/c\hbar = \pi/2$.

angle in this limit that must be compared with scattering theory. The conclusion here is that the scattering consists completely of forward scattering.

The authors are convinced that the Feynman path integral method is incompatible with the assumptions on which the derivation of the Aharonov-Bohm scattering cross section is based. The authors are furthermore convinced that the results of the Feynman path integral method are the correct ones. The wavefunctions that are consistent with the Feynman propragator are the ones discussed by one of us in 1981 [14].

References

[1] Aharonov Y and Bohm D 1959 *Phys. Rev.* **115** 485
[2] Moellenstedt G and Bayh W 1962 *Phys.* Bl **18** 299
[3] Tonomura A, Osakabe N, Matsuda T, Kawasahi T, Endo J, Yano S and Yamada H 1986 *Phys. Rev. Lett.* **56** 792
[4] Tonomura A, Umeyaki H, Matsuda T, Osakabe N, Endo J and Sugita Y *Phys. Rev. Lett.* **48** 331
[5] Feynman R P 1948 *Rev. Mod. Phys.* **20** 267
[6] Feynman R P and Hibbs A 1965 *Quantum Mechanics and Path Integrals* (New York: McGraw-Hill)
[7] Schulman L S 1971 *J. Math. Phys.* **12** 304
[8] Kobe D H 1979 *Ann. Phys.* **123** 381
[9] Inomata A 1987 *Proc. 2nd Int. Symp. on Foundations of Quantum Mechanics* (Physical Society of Japan) p 132
[10] Ohnuki Y 1987 *Proc. 2nd Int. Symp. on Foundations of Quantum Mechanics* (Physical Society of Japan) p 117
[11] Feynman R P and Hibbs A 1965 *Quantum Mechanics and Path Integrals* (New York: McGraw-Hill) pp 47-56
[12] Ralston A and Will A 1967 *Mathematical Methods for Digital Computers* (New York: Wiley) 133-43
[13] Aharonov Y and Bohm D 1959 *Phys. Rev.* **115** 489
[14] Henneberger W C 1981 *J. Math. Phys.* **22** 116